Dissection of SNARE-driven membrane fusion and neuroexocytosis by wedging small hydrophobic molecules into the SNARE zipper

Yoosoo Yang[a,1], Jae Yoon Shin[a,1], Jung-Mi Oh[a], Chang Hwa Jung[a], Yunha Hwang[a], Sehyun Kim[a], Jun-Seob Kim[a], Kee-Jung Yoon[a], Ji-Young Ryu[b], Jaeil Shin[c], Jae Sung Hwang[d], Tae-Young Yoon[b], Yeon-Kyun Shin[c,e,2], and Dae-Hyuk Kweon[a,2]

[a]School of Life Science and Biotechnology and Center for Human Interface Nanotechnology, Sungkyunkwan University, Suwon 440-746, South Korea; [b]Department of Physics, Korea Advanced Institute of Science and Technology (KAIST), Daejeon 760-749, South Korea; [c]Department of Biochemistry, Biophysics, and Molecular Biology, Iowa State University, Ames, IA 50011; [d]Skin Biotechnology Center, Graduate School of Biotechnology and Institute of Life Science and Resources, Kyung Hee University, Yongin 446-701, Korea; and [e]Integrative Biology and Biotechnology, Pohang University of Science and Technology (POSTECH), Pohang 790-784, Korea

Edited by Josep Rizo, University of Texas Southwestern Medical Center, Dallas, TX, and accepted by the Editorial Board November 8, 2010 (received for review May 18, 2010)

Neuronal SNARE proteins mediate neurotransmitter release at the synapse by facilitating the fusion of vesicles to the presynaptic plasma membrane. Cognate v-SNAREs and t-SNAREs from the vesicle and the plasma membrane, respectively, zip up and bring about the apposition of two membranes attached at the C-terminal ends. Here, we demonstrate that SNARE zippering can be modulated in the midways by wedging with small hydrophobic molecules. Myricetin, which intercalated into the hydrophobic inner core near the middle of the SNARE complex, stopped SNARE zippering in motion and accumulated the *trans*-complex, where the N-terminal region of v-SNARE VAMP2 is in the coiled coil with the frayed C-terminal region. Delphinidin and cyanidin inhibited N-terminal nucleation of SNARE zippering. Neuronal SNARE complex in PC12 cells showed the same pattern of vulnerability to small hydrophobic molecules. We propose that the half-zipped *trans*-SNARE complex is a crucial intermediate waiting for a calcium trigger that leads to fusion pore opening.

polyphenol | hemifusion | neurotransmission | neuron

Neurotransmitter release at the synapse, which serves as the brain's major form of cell–cell communication, requires the fusion of synaptic vesicles with the presynaptic plasma membrane. Soluble *N*-ethylmaleimide-sensitive factor attachment protein receptor (SNARE) proteins mediate this synaptic fusion event (1–5), and the formation of a four-helical bundle (6–8) is believed to generate the force required for fusion. A zipper model has been proposed for SNARE complex formation, initiating assembly at the N-terminal region and zipping toward the C-terminal membrane-proximal region (6–9). To account for fast neuroexocytosis, the SNAREs in primed readily releasable vesicles have been proposed as being partially zipped in the *trans*-configuration bridging the two membranes.

Although the structure of the fully assembled *cis*-SNARE complex, which is believed to represent the postfusion state, has been determined (10), the structure of the *trans*-complex is poorly understood and is purely imaginary, most likely because of its inherently transient nature. Precisely linking the degrees of SNARE zippering to specific stages of membrane fusion seems to be prerequisite for determining the structure of the *trans*-complex and for providing answers to the questions of how fast fusion is controlled in neurons and how the *trans*-complexes set up the readily releasable vesicles with other regulatory proteins.

Here, we show that certain small hydrophobic molecules (SHM) enable layer-by-layer control of SNARE zippering by wedging into various points of the SNARE zipper. SNARE-mediated membrane fusion is dissected via this wedge-like action of SHMs. Analysis of the captured replication fork-like structure allowed us to understand the basic architecture of the putative *trans*-complex.

Results

SNARE-Driven Membrane Fusion Can Be Controlled by SHMs with Different Modes of Action. As an initial step to examine the feasibility of whether SHM works as a wedge for the SNARE zippering, 39 polyphenolic compounds representing 12 subgroups were screened for inhibitory activity against SNARE-driven proteoliposome fusion (11). We used polyphenolic compounds as a source for SHM because they are abundant in nature and are known to be versatile in helical bundle binding (12–15). The SHMs displayed a wide range of inhibitory activity during the initial screen, which was conducted at a concentration of 20 μM, equivalent to the concentration of t-SNARE proteins used in the fusion assay (Table S1). The nine most effective compounds were selected for subsequent experiments, and the least effective compound, kaempferol, was used as a negative control. Next, the degree of inhibition of lipid mixing (Fig. 1*A*) and SNARE complex formation (Fig. 1*B*) were determined for each compound at a concentration of 10 μM. The extent of SNARE complex formation was assessed by exploiting the SDS-resistant property of the core complex (16). For all 10 compounds tested, the degree of SNARE complex formation inhibition correlated well with that of lipid-mixing inhibition (Fig. 1*C*), suggesting that SHM-mediated inhibition of membrane fusion is likely a direct consequence of inhibition of SNARE zippering. The tested compounds did not cause liposome fusion without SNARE proteins and did not cause precipitation of proteoliposomes at the concentrations tested (Fig. S1*A*). We exclude the possibility that SHMs inhibited anti-SNAP-25 antibody binding to SNARE complexes (Fig. S1*B*). Thus, the results of the in vitro fusion assay indicate that certain SHMs are capable of down-regulating SNARE complex formation, thereby inhibiting membrane fusion in a concentration-dependent manner (Fig. S1*C*).

Author contributions: Y.Y., T.-Y.Y., Y.-K.S., and D.-H.K. designed research; Y.Y., J.Y.S., J.-M.O., C.H.J., Y.H., S.K., J.-S.K., J.-Y.R., and J.S. performed research; J.Y.S., C.H.J., K.-J.Y., J.-Y.R., and J.S.H. contributed new reagents/analytic tools; Y.Y., Y.-K.S., and D.-H.K. analyzed data; and T.-Y.Y., Y.-K.S., and D.-H.K. wrote the paper.

The authors declare no conflict of interest.

This article is a PNAS Direct Submission. J.R. is a guest editor invited by the Editorial Board.

[1]Y.Y. and J.Y.S. contributed equally to this work.

[2]To whom correspondence may be addressed. E-mail: colishin@iastate.edu or dhkweon@skku.edu.

This article contains supporting information online at www.pnas.org/lookup/suppl/doi:10.1073/pnas.1006899108/-/DCSupplemental.

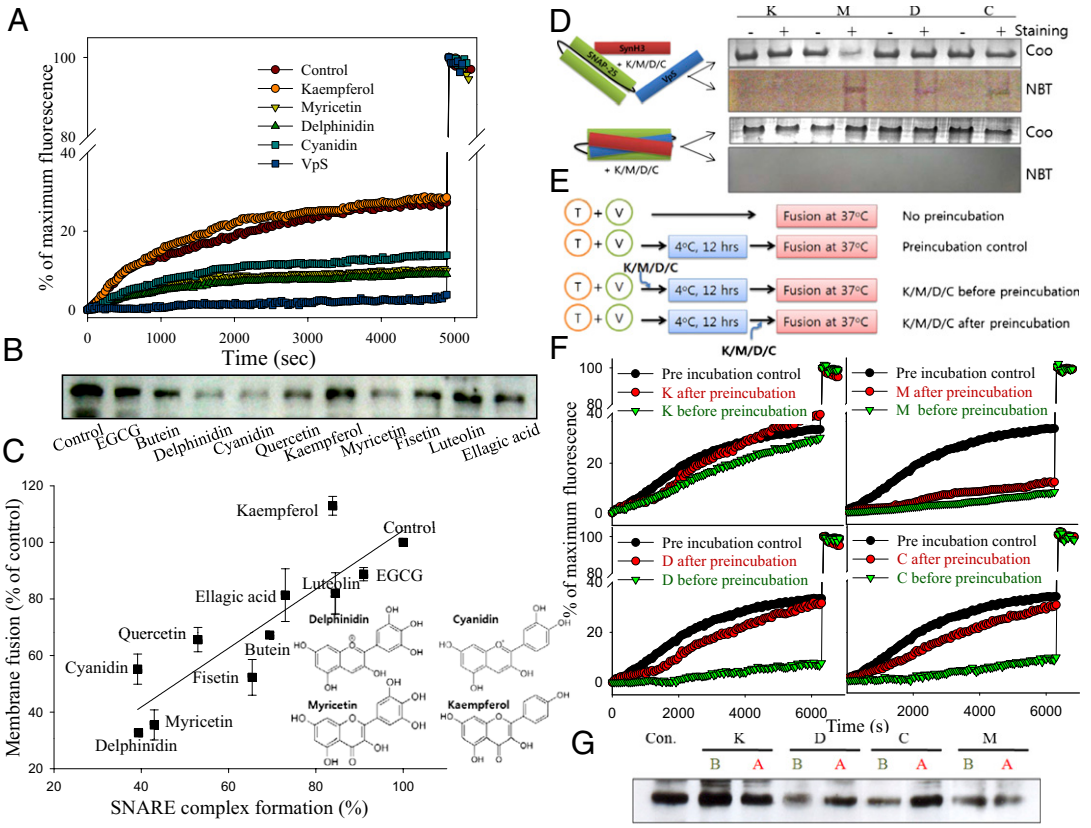

Fig. 1. Down-regulation of SNARE-driven membrane fusion by SHMs. (*A*) Percentage maximum fluorescence intensity was plotted as a function of time in the presence or absence of SHMs. VpS, the soluble domain of VAMP2 lacking the transmembrane domain. SHMs were added at 10 μM concentration. (*B*) SNARE complex formation was assessed after the membrane-fusion assay by Western blotting using anti-SNAP25 antibody. (*C*) Correlation between the degree of membrane fusion and the amount of SNARE complex formed in the presence or absence of SHMs. The concentration of SHM was 10 μM, and the degree of fusion and complex formation were determined after an 80-min fusion initiation. Chemical structures of delphinidin, cyanidin, myricetin, and kaempferol are shown in the *Inset*. Concentration-dependent inhibition of fusion by these four SHMs is shown in Fig. S1C. (*D*) Soluble SNARE motifs form SDS-resistant complexes with SHMs in the inner layer. In the upper two gels, soluble fragments of SNARE proteins (each 500 μg/mL) were mixed with 10 μM SHMs and separated by SDS/PAGE. Gels were either stained with Coomassie blue (Coo) or electroblotted onto nitrocellulose membrane followed by incubation with nitroblue tetrazolium. + and − indicate the presence or absence of SHMs, respectively. In the lower two gels, the same experiment was performed with preformed core complexes. Results indicate that SHMs bind to inner layer of the SNARE complex. K, kaempferol; M, myricetin; D, delphinidin; C, cyanidin. (*E*) Experimental procedures to determine fusion step-specific effects of SHMs on membrane fusion. (*F*) Fusion step-specific effects of SHMs on membrane fusion. (*G*) Western blot analysis of SNARE complex formation. B, addition of SHMs before preincubation; A, addition of SHMs after preincubation.

We performed further experiments using the three most efficient compounds, delphinidin, cyanidin, and myricetin, as well as the least effective, kaempferol (insets in Fig. 1*C*). First, by using soluble SNARE motifs, SHMs were shown to intercalate into the inner layer of the SNARE complex. SNARE complex-bound SHMs were detected by nitroblue tetrazolium staining, which allows colorimetric detection of protein-bound polyphenols, only when the SHMs were added before complex formation, indicating that the inhibitory SHMs intercalate into the inner layer of the core complex during helical bundle formation (Fig. 1*D*). The SHMs did not bind to binary t-SNARE complex regardless of the presence or absence of the Habc domain and transmembrane domain of syntaxin 1 (Fig. S2).

To gain further insight into the mechanism by which SHMs inhibit membrane fusion, the fusion step-specific effect on SNARE-dependent proteoliposome fusion was examined (17). Preincubation of t- and v-SNARE vesicle mixtures at 4 °C is known to enrich N-terminal, partially zipped complex and enhance membrane fusion when the temperature is subsequently elevated to 37 °C. SHMs were added to the reaction either before or after this preincubation step (Fig. 1*E*). SNARE-mediated fusion was dramatically reduced when myricetin, delphinidin, or cyanidin was added before the preincubation step, whereas kaempferol had only a slight effect (Fig. 1*F*). In contrast, when the SHMs were introduced after the preincubation step, the effects became divergent. Myricetin largely retained its inhibitory activity, whereas delphinidin and cyanidin showed little inhibitory effect. The amount of SNARE complex formed correlated well with the results of the lipid-mixing assay (Fig. 1*G*).

Binding Sites of SHMs in the SNARE Complex and the Effect of Differential Binding on Hemifusion. We performed Ala-scanning experiments to locate potential binding region of the three SHMs in the SNARE zipper. All amino acids located at internal *a* and *d* positions of the VAMP2 helix were mutated to alanine one at a time, with the exception of native alanine residues. P20A and P23A mutants were also prepared because the proline-rich region is known to have affinity to some polyphenols (18), and VAMP2 contains the proline-rich region before the SNARE motif. The effect of each Ala mutation was assessed with the in vitro fusion assay (Fig. 2*A*). With only a few exceptions, most Ala mutations hampered SNARE-mediated fusion by ~50%, emphasizing the importance of the conserved core residues for the fusion activity. The Ala mutants were then subjected to the lipid-mixing assay in the presence of an SHM. We reasoned that when a binding site for a particular SHM is

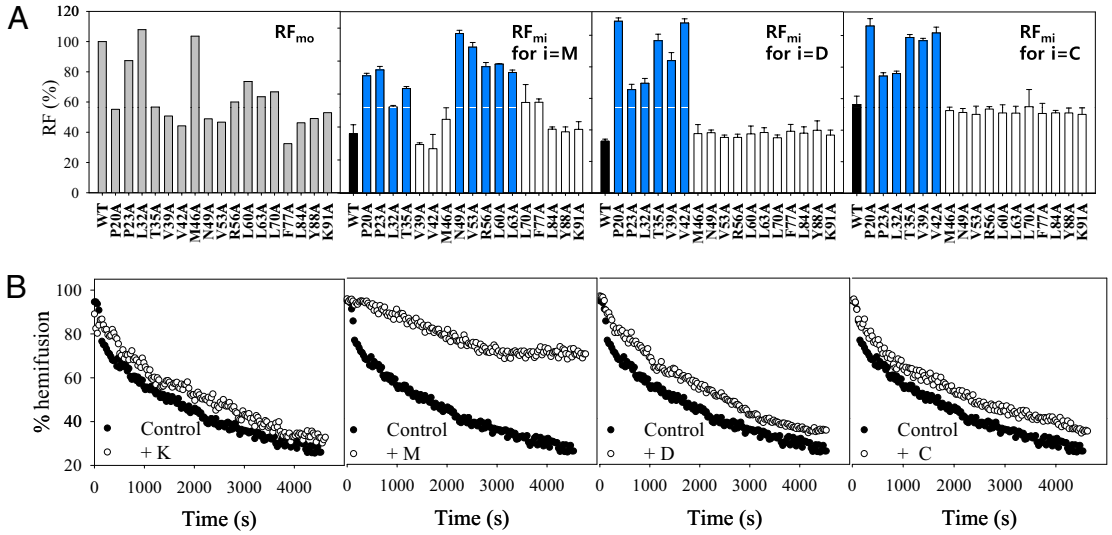

Fig. 2. Determination of SHM wedging points in the SNARE zipper and correlation of the degree of zippering with membrane-fusion stage. (*A*) The effect of alanine mutations on relative fusion efficiency. RF_{mo} denotes the relative fusion efficiency of alanine mutants compared with wild-type VAMP2. RF_{mi} is the ratio between percentage maximum fluorescence intensities obtained in the presence or absence of inhibitors for the same mutant, where the inhibitors are myricetin (M), delphinidin (D), and cyanidin (C) from left to right. The mutations with significantly higher values (blue bars) above RF_{wi} (black bars) indicate that those mutations are not inhibited by the SHM and thus represent the points that the SHM wedges into the SNARE zipper. The first black bar in each set denotes RF_{wi} for each SHM. Equations used to obtain relative fusion efficiency values are described in Fig. S3. (*B*) Percentage hemifusion state was determined through the inner-leaflet mixing assay in the absence or presence of SHMs. The actual time-dependent traces are shown in Fig. S4. each SHM was used at 10 μM in both studies.

mutated to Ala, the mutant would lose ability to bind the SHM, thereby relieving inhibition by that SHM (Fig. S3). The relative fusion efficiency, defined as the ratio between the percentage maximum fluorescence intensity (PMF) measured in the presence of the drug to the PMF measured in the absence of the drug, was plotted along the VAMP2 helix sequence for each SHM. Myricetin appears to have two binding sites: a weak binding site coordinated by hydrophobic residues between residues 20 and 35 of VAMP2 and the corresponding t-SNARE hydrophobic layers and a strong binding site coordinated by the hydrophobic layers in the middle region (residues 49–63 of VAMP2 and the corresponding t-SNARE residues). In contrast, delphinidin and cyanidin both had only one strong binding site at the N-terminal region between residues 20 and 42. These results were consistent with the results from the preincubation experiments. It is noted that the proline-rich region also contributes to SHM binding to the N terminus of SNARE complex, perhaps through hydrophobic interaction (18). Although high-resolution structures of SHM-containing SNARE complexes need to be determined for better understanding of binding mechanisms, we speculate that the proline-rich region caps the N-terminal SNARE bundle to enhance the SHM binding (Fig. S6*E* and Fig. S7).

We hypothesized that it would be possible to link the degree of SNARE zippering to specific stages of membrane fusion by harnessing the unique properties of each SHM. We measured hemifusion by using sodium dithionite that selectively kills fluorescent dyes in outer leaflets (19). Myricetin inhibited inner-leaflet mixing efficiently but allowed outer-leaflet mixing, stalling as much as 80% of the fusion outcome at the hemifusion state (Fig. 2*B*). In contrast, delphinidin and cyanidin had just a slight effect on the fraction of hemifusion (Fig. 2*B* and Fig. S4). Together, our results raise the possibility that myricetin arrests membrane fusion at the hemifusion state by wedging into the middle region of the SNARE zipper.

Overall Fold of the Half-Zipped SNARE Complex. To determine the rough structure of SNARE zipper wedged by myricetin, fluorescence-quenching assays were performed with Cy5-labeled VAMP2 mutants (Fig. 3). Five Cy5-labeled VAMP2 mutants were prepared: Q33C and T35C to probe N-terminal zippering, L54C and R56C for middle region zippering, and D68C for C-terminal zippering. F_O/F, where F_O and F represent fluorescence intensity measured in the absence or presence of the fluorescence quencher acrylamide, respectively, increases if acrylamide is readily accessible to Cy5, indicating the labeled position is frayed. Conversely, the slope is less affected by the quencher when the Cy5-label is positioned in the coiled-coil region. In this regard, preincubation at 4 °C (Fig. 3, scheme A) seems to result in the replication fork-like SNARE zipper, where the N-terminal region of VAMP2 is in the coiled-coil structure and the C-terminal region remains frayed. After membrane fusion at 37 °C (Fig. 3, scheme B), all labeled VAMP2 residues appeared to participate in SNARE complex formation. By contrast, in the presence of myricetin (Fig. 3, scheme D), the fluorescence-quenching pattern was similar to those of scheme A, indicating that SNARE zipper wedged by myricetin has the frayed C terminus.

Dissection of SNARE-Dependent Membrane Fusion in PC12 Cells with SHMs. The next natural question is whether these observations are also true in live cells. First, we tested whether the SHMs could regulate SNARE complex formation in live cells. We prepared NGF-treated PC12 cells loaded with [^{3}H]noradrenaline. Based on the in vitro results, we expected that the SHM binding sites in the SNARE complexes would only be exposed during recycling of SNARE proteins. To induce SNARE recycling, the cells were pretreated with a high concentration of KCl followed by immediate addition of SHMs. A high concentration of KCl is known to induce depolarization of PC12 cells leading to SNARE-mediated membrane fusion and release of neurotransmitters (20).

After high-K^+ pretreatment (Fig. 4*A*, red box), neurotransmitter release was strongly inhibited by SHM exposure (Fig. 4*B*, red bars). The three most competent compounds, delphinidin, cyanidin, and myricetin, showed 75–80% inhibition at 10 μM, comparable to the calcium channel blocker verapamil (21, 22) and only slightly lower than the *Clostridium botulinum* neurotoxin D

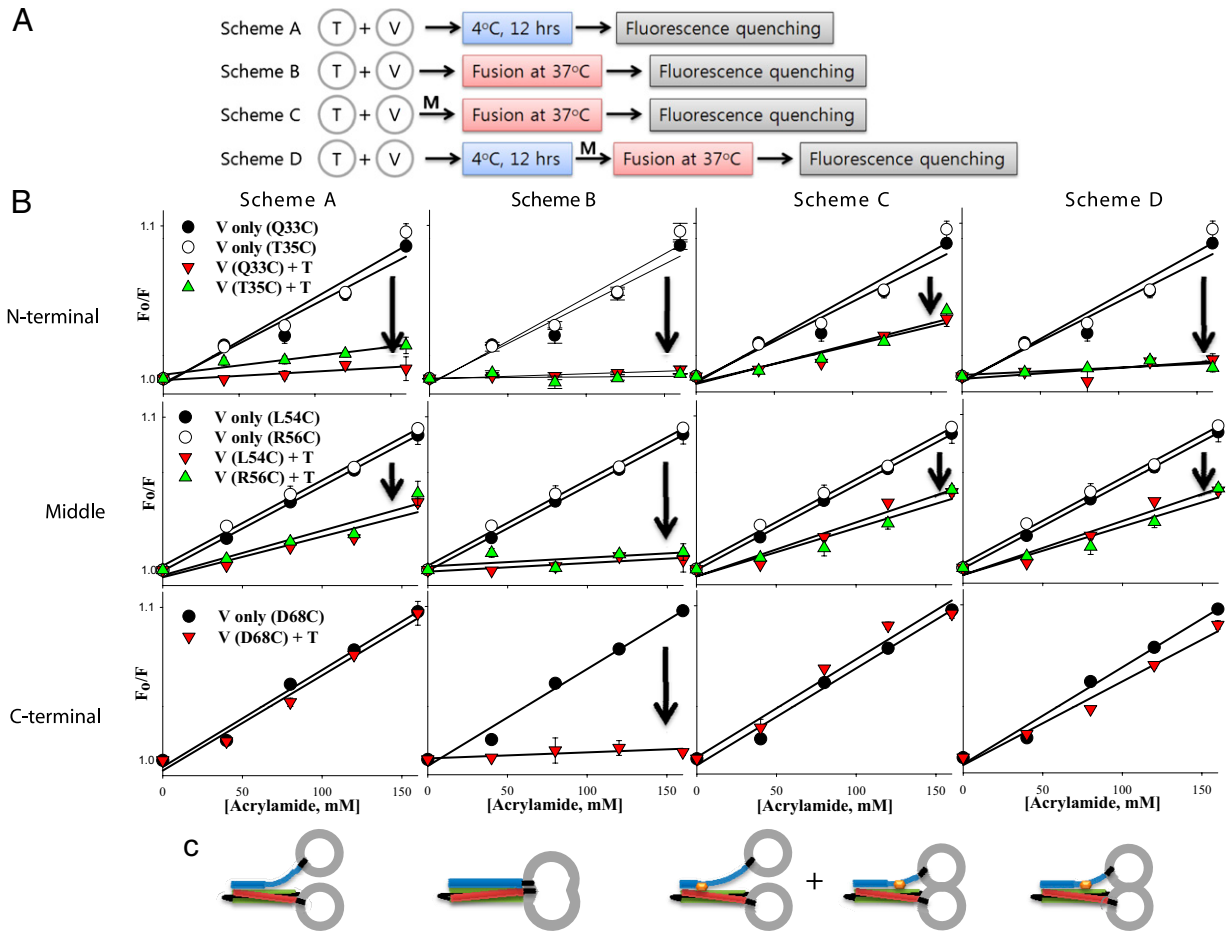

Fig. 3. Fluorescence-quenching experiments for Cy5-labeled VAMP2 mutants. (*A*) Schematic presentation of fluorescence-quenching experiments to determine the structure of the SNARE zipper wedged by myricetin. (*B*) Stern–Volmer plots for the five Cy5-labeled VAMP2 mutants measured under various conditions as indicated in schemes A–D. F_O and F represent fluorescence intensity measured in the absence or presence of the fluorescence quencher acrylamide, respectively. Arrows indicate that the residues are engaged into the coiled-coil region when t-vesicle is present. A smaller difference in quenching efficiency (indicated by short arrows) may result from partial coiling (schemes A and D) or because of a mixture of free VAMP2 and the half-zippered complex (scheme C). (*C*) Structures of SNARE zipper expected from the fluorescence-quenching experiments.

(BoNT/D). This high-K^+ pretreatment experiment appeared to mirror the in vitro preincubation experiment in which SHMs were added before 4 °C preincubation (Fig. 1 *E* and *F*). Alternatively, the in vitro results of adding SHMs after 4 °C preincubation were expected to correspond to those from the neuronal cells without high-K^+ pretreatment (Fig. 4*A*, blue box). Only myricetin showed a significant inhibitory effect on neuroexocytosis (Fig. 4*B*, blue bars), which is consistent with our in vitro observations that myricetin hampered C-terminal zippering by wedging the half-zipped partial complex.

Membrane proteins were extracted from PC12 cells and analyzed by Western blotting using an antibody against SNAP-25 (Fig. 4*C*). Depolarization by high K^+ indeed induced SDS-resistant SNARE complex formation (low K^+ vs. high K^+). In the presence of SHMs, depolarization-induced SNARE complex formation was reduced, which is in agreement with the neurotransmitter release results. Delphinidin and cyanidin effectively reduced SNARE complex formation only when the neuronal cells were pretreated with high-K^+ solution (Fig. 4*C*, red box). In contrast, myricetin effectively reduced SDS-resistant complex formation even without high-K^+ pretreatment (Fig. 4*C*, blue box). Thus, the conformation of the *trans*-SNARE complex in neuronal cells is likely to be similar to that observed in vitro, where the delphinidin- and cyanidin-binding sites are concealed inside the N-terminal bundle and the C-terminal stronger myricetin-binding site is not yet zipped.

Discussion

In the present study, it was shown that dynamic SNARE zippering process could be stopped at the point of interest by wedging an appropriate SHM into the zipper. Delphinidin and cyanidin wedge into the SNARE zipper at the far N terminus (~P20–V42 of VAMP2), thereby preventing N-terminal nucleation of SNARE complex formation (Fig. S8*F*). Myricetin stops subsequent C-terminal zippering by wedging into the middle region of the SNARE zipper after the N-terminal half is zipped (Fig. S8*G*). By harnessing these unique characteristics of SHMs, we dissected SNARE-driven membrane fusion and tried to link the degree of SNARE zippering to the specific membrane-fusion intermediates.

Preincubation at 4 °C is known to enhance membrane fusion at the subsequently elevated temperature. This preincubation step is thought to accumulate the N-terminal partial complexes (Fig. S8*A*), which undergo complete zippering in a synchronized manner when the temperature is raised (11). When t-vesicles were mixed with vesicles containing Cy5-labeled VAMP2 at 4 °C, we could confirm the formation of the N-terminal partial complex with frayed C-terminal SNARE motifs (Fig. 3). The partial

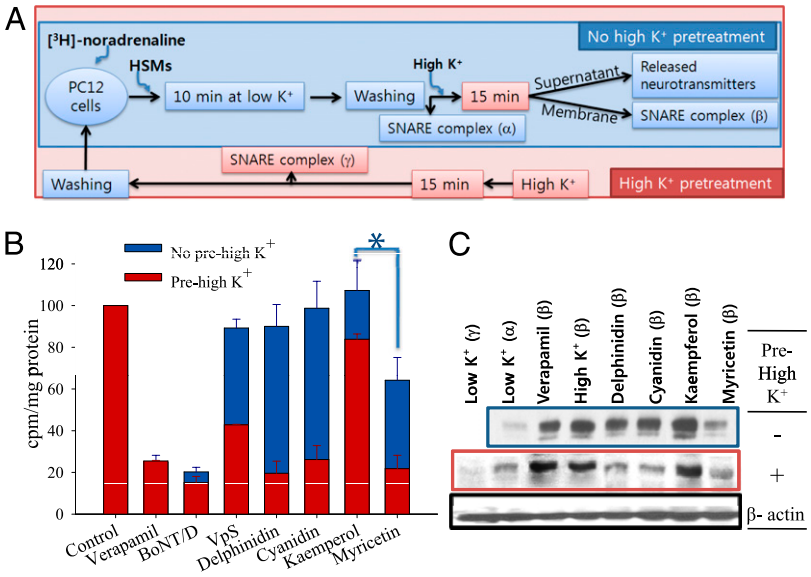

Fig. 4. The effect of SHMs on neurotransmitter release and SNARE complex formation. (*A*) Experimental procedures. Red box, high-K^+ pretreatment; blue box, no pretreatment. (*B* and *C*) After 15 min of main high-K^+-induced depolarization, the amount of released neurotransmitters (*B*) and the amount of SDS-resistant SNARE complexes (*C*) were quantified in the supernatant and membrane fraction, respectively. α, β, and γ indicate the time of sampling for membrane fraction as shown in *A*. Reduced band intensity indicated by γ compared with β in the red-boxed gel shows that the pretreatment of high K^+ effectively dissembles preexisting SDS-resistant SNARE complexes in the cells. Red, high-K^+ pretreatment group; blue, no pretreatment group. The effect of SHMs on cell viability is shown in Fig. S5 *A* and *B*. IC_{50} values of SHMs on neurotransmitter release are shown in Fig. S5*C*. Statistical significance of differences was evaluated by ANOVA (*$P < 0.05$).

complex, however, has never been captured at physiological temperatures. The arrested zippering at physiological temperature by myricetin provides information about the *trans*-complex. Because the myricetin binding site is predicted to be coordinated by the hydrophobic residues of VAMP2 ~N49–L63 and corresponding t-SNARE residues (Fig. 2*A*), and the partial complex formed by 4 °C preincubation is susceptible to myricetin (Fig. 1 *E*–*G*), the results suggested that the region of VAMP2 after N49 remains unzipped in the partial complex. Because this partial complex is not susceptible to delphinidin or cyanidin, which bind before V42, the SHMs-assisted assays suggest the possibility that the N-terminal region up to M46 forms a coiled coil during 4 °C preincubation. Static fluorescence-quenching experiments (Fig. 3) also support that this halfway N-terminal zippering up to M46 with the frayed C-terminal half of VAMP2 is likely to represent the *trans*-complex (Fig. S8*D′*).

It is believed that SNARE complex formation starts at the membrane-distal N-terminal region and zips toward the membrane-proximal C-terminal region (6–9), thereby effectively forcing the apposition of the two membranes. Also, it is widely accepted that N-terminal assembly of SNARE proteins underlies vesicle priming, whereas assembly of the C-terminal end drives fusion. In this model, an intermediate state of the SNARE complex is associated with the primed vesicle state, and subsequent C-terminal assembly, assisted by other proteins such as synaptotagmin and complexin, leads to membrane fusion and the relaxation of *trans*-SNAREpins into *cis*-SNARE complexes. Many of recent studies on complexin- and synaptotagmin-modulated fast neuroexocytosis presume this model to be true to account for their findings (3, 10, 23–27). However, our results raise another possibility, where N-terminal half zippering, which had been merely considered responsible for vesicle docking, might be sufficient to induce hemifusion and is the minimal zippering degree for membrane hemifusion. Our results suggest that the zippering degree responsible for hemifusion could be only up to residue 46 of VAMP2 (Fig. S8*D*).

Evidence indicates that the hemifusion state is a stable intermediate of exocytosis in neuronal cells in vivo (28), and two membranes may be hemifused before Ca^{2+} influx (29, 30). The similar responses to SHM treatments observed in both reconstituted proteoliposomes and neuronal PC12 cells suggest that the halfway zippering-mediated hemifusion state (Fig. S8*G*) may be also true in the neuron. The hemifusion state likely progresses toward the fusion pore when calcium triggers full SNARE zippering (Fig. S8*E*), with the help of other regulatory proteins such as synaptotagmin and complexin (31). We note, however, that there are contradictory results against the hemifusion state (32), and there is the possibility, although unlikely, that myricetin's interaction with the membrane is in part responsible for hemifusion arrest (Fig. S7).

BoNTs elicit neuron-specific flaccid paralysis by specifically cleaving neuronal SNARE proteins. After the realization of the therapeutic potentials of these otherwise fatal toxins, the Food and Drug Administration approved the controlled use of BoNT/A for the treatment of several hypersecretion-related neurological diseases, such as strabismus, blepharospam, hemifacial spasm, and cervical dystonia (33). Recently, the cosmetic use of these toxins for treating glabellar facial lines and axillary hyperhidrosis has gained immense popularity. Can small molecules, with more conventional drug-like properties, also regulate SNARE complex formation and consequent neuroexocytosis? Promisingly, our results imply that SNARE-wedging small molecules might serve as SNARE-specific drugs, which will definitely provide a tractable avenue in treating a variety of human hypersecretion diseases. These small molecules can serve as general chemical platforms from which unique and potent SNARE-specific drugs can be derived.

Materials and Methods

Materials. 1-Palmitoyl-2-dioleoyl-*sn*-glycero-3-phosphatidylcholine (POPC), 1,2-dioleoyl-*sn*-glycero-3-phosphatidylserine (DOPS), 1,2-dioleoyl-*sn*-glycero-3-phosphoserine-*N*-(7-nitro-2-1,3-benzoxadiazol-4-yl) (NBD-PS), and 1,2-dioleoyl-*sn*-glycero-3-phosphoethanolamine-*N*-(lissamine rhodamine B sulfonyl) (rhodamine-PE) were obtained from Avanti Polar Lipids. RPMI medium 1640,

penicillin-streptomycin, horse serum, and FBS were purchased from GIBCO/BRL. Recombinant BoNT/D light chain was purchased from List Biological Laboratories. All other chemicals, including polyphenolic compounds, were purchased from Sigma-Aldrich.

PC12 Cell Culture and Determination of [^{3}H]Noradrenaline Release. PC12 cells were purchased from the Korean Cell Line Bank (Seoul, Korea). The PC12 cells were plated onto poly-D-lysine–coated culture dishes and were maintained in RPMI medium 1640 containing 100 μg/mL streptomycin, 100 U/mL penicillin, 2 mM L-glutamine, and 10% heat-inactivated FBS at 37 °C in a 5% CO_2 incubator. The cell cultures were split once a week, and the medium was refreshed three times a week. PC12 cells were treated with NGF (7S, 50 ng/mL, Invitrogen) for 5 d before uptake and release of [^{3}H] noradrenaline.

After NGF-treated PC12 cells were grown in 12-well plates at a density of 4×10^5 cells per dish, small-molecule compounds (10 μM) and [^{3}H]noradrenaline (1 μCi/mL) were applied for 10 min in low-K^+ solution (140 mM NaCl, 4.7 mM KCl, 1.2 mM KH_2PO_4, 2.5 mM $CaCl_2$, 1.2 mM $MgSO_4$, 11 mM glucose, and 15 mM Hepes-Tris, pH 7.4). The cells were washed four times to remove the unincorporated radiolabeled neurotransmitters. The cells were then depolarized with a high-K^+ solution (115 mM NaCl, 50 mM KCl, 1.2 mM KH_2PO_4, 2.5 mM $CaCl_2$, 1.2 mM $MgSO_4$, 11 mM glucose, and 15 mM Hepes-Tris, pH 7.4) for 15 min to assess the stimulated release. Extracellular media was transferred to scintillation vials and measured by liquid scintillation counting. The quantity of released neurotransmitter was calculated according to the following equation: The quantity of released [^{3}H]noradrenaline = (cpm of high-K^+-stimulated sample − cpm of basal level release)/mg of protein. The amount of secreted neurotransmitters was determined without pretreatment of detergents for permeabilization except for VpS and BoNT/D. Cell permeabilization for incorporation of VpS and BoNT/D (5 nM) was accomplished with 10 μM digitonin in low-K^+ solution (34). For high-K^+ pretreatment groups, polyphenols were not added before the first high-K^+ treatment but were before the second high-K^+ treatment.

Statistical Analysis. All experimental data were examined by ANOVA procedures, and significant differences among the means from three to five repeats were assessed with Duncan's multiple range tests and the Statistical Analysis System, version 8.2 (SAS Institute).

ACKNOWLEDGMENTS. This work was supported by the Basic Science Research Program (2007-D00243 and 2010-0015035), by the Mid-Career Researcher Program (2009-0058612), and by the World Class University Program through the National Research Foundation of Korea. This work was also supported by Amorepacific Corporation and Small and Medium Business Administration.

1. Söllner T, et al. (1993) SNAP receptors implicated in vesicle targeting and fusion. *Nature* 362:318–324.
2. Rizo J, Rosenmund C (2008) Synaptic vesicle fusion. *Nat Struct Mol Biol* 15:665–674.
3. Südhof TC, Rothman JE (2009) Membrane fusion: Grappling with SNARE and SM proteins. *Science* 323:474–477.
4. McNew JA (2008) Regulation of SNARE-mediated membrane fusion during exocytosis. *Chem Rev* 108:1669–1686.
5. Sørensen JB (2005) SNARE complexes prepare for membrane fusion. *Trends Neurosci* 28:453–455.
6. Fiebig KM, Rice LM, Pollock E, Brunger AT (1999) Folding intermediates of SNARE complex assembly. *Nat Struct Biol* 6:117–123.
7. Chen YA, Scales SJ, Scheller RH (2001) Sequential SNARE assembly underlies priming and triggering of exocytosis. *Neuron* 30:161–170.
8. Melia TJ, et al. (2002) Regulation of membrane fusion by the membrane-proximal coil of the t-SNARE during zippering of SNAREpins. *J Cell Biol* 158:929–940.
9. Ellena JF, et al. (2009) Dynamic structure of lipid-bound synaptobrevin suggests a nucleation-propagation mechanism for *trans*-SNARE complex formation. *Proc Natl Acad Sci USA* 106:20306–20311.
10. Stein A, Weber G, Wahl MC, Jahn R (2009) Helical extension of the neuronal SNARE complex into the membrane. *Nature* 460:525–528.
11. Weber T, et al. (1998) SNAREpins: Minimal machinery for membrane fusion. *Cell* 92: 759–772.
12. Liu S, Wu S, Jiang S (2007) HIV entry inhibitors targeting gp41: From polypeptides to small-molecule compounds. *Curr Pharm Des* 13:143–162.
13. Cai L, Gochin M (2007) A novel fluorescence intensity screening assay identifies new low-molecular-weight inhibitors of the gp41 coiled-coil domain of human immunodeficiency virus type 1. *Antimicrob Agents Chemother* 51:2388–2395.
14. Frey G, et al. (2006) Small molecules that bind the inner core of gp41 and inhibit HIV envelope-mediated fusion. *Proc Natl Acad Sci USA* 103:13938–13943.
15. Cooper WJ, Waters ML (2005) Molecular recognition with designed peptides and proteins. *Curr Opin Chem Biol* 9:627–631.
16. Otto H, Hanson PI, Jahn R (1997) Assembly and disassembly of a ternary complex of synaptobrevin, syntaxin, and SNAP-25 in the membrane of synaptic vesicles. *Proc Natl Acad Sci USA* 94:6197–6201.
17. Shen J, Tareste DC, Paumet F, Rothman JE, Melia TJ (2007) Selective activation of cognate SNAREpins by Sec1/Munc18 proteins. *Cell* 128:183–195.
18. Hagerman AE, Butler LG (1981) The specificity of proanthocyanidin-protein interactions. *J Biol Chem* 256:4494–4497.
19. Lu X, Zhang F, McNew JA, Shin YK (2005) Membrane fusion induced by neuronal SNAREs transits through hemifusion. *J Biol Chem* 280:30538–30541.
20. Ray P, Berman JD, Middleton W, Brendle J (1993) Botulinum toxin inhibits arachidonic acid release associated with acetylcholine release from PC12 cells. *J Biol Chem* 268: 11057–11064.
21. Hay DW, Wadsworth RM (1983) The effects of calcium channel inhibitors and other procedures affecting calcium translocation on drug-induced rhythmic contractions in the rat vas deferens. *Br J Pharmacol* 79:347–362.
22. Richardson CM, Dowdall MJ, Bowman D (1996) Inhibition of acetylcholine release from presynaptic terminals of skate electric organ by calcium channel antagonists: A detailed pharmacological study. *Neuropharmacology* 35:1537–1546.
23. McMahon HT, Kozlov MM, Martens S (2010) Membrane curvature in synaptic vesicle fusion and beyond. *Cell* 140:601–605.
24. Rizo J (2010) Synaptotagmin-SNARE coupling enlightened. *Nat Struct Mol Biol* 17: 260–262.
25. Matos MF, Mukherjee K, Chen X, Rizo J, Südhof TC (2003) Evidence for SNARE zippering during Ca^{2+}-triggered exocytosis in PC12 cells. *Neuropharmacology* 45: 777–786.
26. Maximov A, Tang J, Yang X, Pang ZP, Südhof TC (2009) Complexin controls the force transfer from SNARE complexes to membranes in fusion. *Science* 323:516–521.
27. Xue M, et al. (2010) Binding of the complexin N terminus to the SNARE complex potentiates synaptic-vesicle fusogenicity. *Nat Struct Mol Biol* 17:568–575.
28. Wong JL, Koppel DE, Cowan AE, Wessel GM (2007) Membrane hemifusion is a stable intermediate of exocytosis. *Dev Cell* 12:653–659.
29. Zampighi GA, et al. (2006) Conical electron tomography of a chemical synapse: Vesicles docked to the active zone are hemi-fused. *Biophys J* 91:2910–2918.
30. Vrljic M, et al. (2010) Molecular mechanism of the synaptotagmin-SNARE interaction in Ca^{2+}-triggered vesicle fusion. *Nat Struct Mol Biol* 17:325–331.
31. Schaub JR, Lu X, Doneske B, Shin YK, McNew JA (2006) Hemifusion arrest by complexin is relieved by Ca^{2+}-synaptotagmin I. *Nat Struct Mol Biol* 13:748–750.
32. Fernández-Busnadiego R, et al. (2010) Quantitative analysis of the native presynaptic cytomatrix by cryoelectron tomography. *J Cell Biol* 188:145–156.
33. Dolly JO, Lawrence GW, Meng J, Wang J, Ovsepian SV (2009) Neuro-exocytosis: Botulinum toxins as inhibitory probes and versatile therapeutics. *Curr Opin Pharmacol* 9:326–335.
34. Jung CH, et al. (2008) A search for synthetic peptides that inhibit soluble *N*-ethylmaleimide sensitive-factor attachment receptor-mediated membrane fusion. *FEBS J* 275:3051–3063.